THE ASTROPHYSICAL JOURNAL, 428:377–383, 1994 June 10

FAR-INFRARED LINE MAPPER (FILM) ON THE INFRARED TELESCOPE IN SPACE

HIROSHI SHIBAI,[1] MASAO YUI,[1,2] HIDEO MATSUHARA,[3] NORIHISA HIROMOTO,[4]
TAKAO NAKAGAWA,[1] AND HARUYUKI OKUDA[1]
Received 1993 April 8; accepted 1993 December 10

ABSTRACT

We have developed a Far-Infrared Line Mapper (FILM) as one of the four focal plane instruments on the Infrared Telescope in Space (IRTS). The FILM is a grating spectrometer designed to simultaneously measure [C II] 158 μm and [O I] 63 μm line intensities and continuum emission near the [C II] line with spatial resolution of 8 arcmin. Very high sensitivity and accuracy are achieved by using stressed and unstressed Ge:Ga detectors at 1.8 K with a helium cooled telescope and by using a spectral scanner to distinguish the line emission from the continuum emission. Line intensities of the [C II] and the [O I] will be mapped over 10% of the sky with much higher sensitivity than the previous survey measurements.

Subject headings: artificial satellites, space probes — infrared: general — instrumentation: spectrograph

1. INTRODUCTION

The far-infrared wavelength region is heavily obscured by the Earth's atmosphere. In order to measure astronomical far-infrared radiation, we must lift up the instruments to the stratosphere at least. The *Infrared Astronomical Satellite* (*IRAS*) has mapped the far-infrared continuum radiation with high sensitivity and high spatial resolution over the entire sky. On the other hand, spectroscopic measurements using balloons and aircraft have not been extended over wider area of the sky such as the Galactic plane.

Recently, two balloon projects, the Balloon-Borne Infrared Telescope (BIRT) and the Balloon-Borne Infrared Carbon Explorer (BICE), have succeeded in making line intensity maps of [C II] 158 μm of the Galactic plane (Shibai et al. 1991; Nakagawa et al. 1993), M17 complex (Matsuhara et al. 1992), the Galactic center (Okuda et al. 1989), and Cygnus-X region (Doi et al. 1993) with good spatial resolution and wide sky coverage. It has been demonstrated by their observational results that measurements of the [C II] line emission are important and powerful tools for investigating the interstellar gas.

On the other hand, the *Cosmic Background Explorer* (*COBE*) has provided all sky intensity maps of [C II] 158 μm and [N II] 205 μm (Wright et al. 1991). The maps reveal an entire view of the Galactic interstellar gas. However, because of its large beam size of 7°, the maps do not have enough spatial resolution to resolve the Galactic plane.

This paper describes the Far-Infrared Line Mapper (FILM), which has been developed to be the first satellite-borne instrument optimized to map far-infrared line intensities. It is an order of magnitude more sensitive than the balloon-borne instruments, has a better spatial resolution than the *COBE*, and will survey a wider sky coverage than the ISO-LWS (Infrared Space Observatory—Long Wavelength Spectrometer).

[1] The Institute of Space and Astronautical Science (ISAS), Yoshino-dai 3-1-1, Sagamihara, Kanagawa 229, Japan.
[2] The Faculty of Science, The University of Tokyo, Yayoi 2-11-16, Bunkyo-ku, Tokyo 113, Japan.
[3] The Faculty of Science, Nagoya University, Hurocho, Chikusa-ku, Nagoya 464, Japan.
[4] Communications Research Laboratory (CRL), Nukui-kitamachi 4-2-1, Koganei, Tokyo 184, Japan.

The FILM is one of the four focal plane instruments of the Infrared Telescope in Space (IRTS) (Murakami et al. 1994). The IRTS is one of the 11 experiments of the Japanese Space Flyer Unit (SFU) which will be launched in early 1995. The IRTS is a 15 cm liquid helium cooled telescope that will survey approximately 10% of the sky during its three-week mission. Other focal plane instruments are a Near-Infrared Spectrometer (NIRS) (Noda et al. 1994), a Mid-Infrared Spectrometer (MIRS), (Roellig et al. 1994), and a Far-Infrared Photometer (FIRP) (Lange et al. 1994).

2. SCIENTIFIC GOALS

The FILM is aimed to investigate far-infrared line emissions of [C II] ($^2P_{3/2}$–$^2P_{1/2}$) 157.7408 μm (Cooksy, Blake, & Saykally 1986) and [O I] ($^3P_1$–$^3P_2$) 63.1837 μm (Zink et al. 1991) from extended sources described below.

2.1. *Origin of the Diffuse* [C II] *Emission*

It has been shown that, in interstellar space, the carbon atom tends to be singly ionized by ultraviolet (UV) photons coming from early-type stars (the ionization potential is 11.26 eV) and that the C^+ ion provides the most important process by the [C II] 158 μm line emission for cooling of the gas (Pottasch, Wesselius, & van Duinen 1979; Tielens & Hollenbach 1985; van Dishoeck & Black 1988).

Stacey et al. (1985) detected the extended [C II] emission from the Galactic plane. Shibai et al. (1991) confirmed the [C II] emission is extended and strong everywhere in the Galactic plane between $l = 30°$ and 51° and that the [C II] emission probably comes from "diffuse photodissociation regions" surrounding giant molecular clouds. The derived total luminosity of the [C II] emission is 3×10^7 $L_\odot$ for the inner Galactic plane and the derived mass fraction of the C^+ region is 30%–50% of that of the molecular mass traced by CO ($J = 1$–0). These observational results have been confirmed by a recent complete [C II] survey of the Galactic plane (Nakagawa et al. 1993). Wright et al. (1991) also reported the total Galactic luminosities of nine far-infrared lines including [C II].

The origin of the diffuse [C II] component, however, has not yet been explained. It is still unknown whether the emission originates in neutral gas clouds where the temperature is 100–

300 K and the density is 100–1000 cm^{-3}, or in extended low-density (ELD) H II regions where the temperature is 5000–10,000 K and the density is 1–10 cm^{-3}.

Unlike carbon, the ionization potential of oxygen is approximately equal to that of hydrogen. Hence neutral oxygen does not exist in the ELD H II regions. In low-density (~ 100 cm^{-3}) photodissociation regions, the [O I] intensity is expected to be 10–100 times smaller than the [C II] intensity (Hollenbach, Takahashi, & Tielens 1991). The observed [C II] intensity at the ridge of the Galactic plane is approximately a few times 10^{-4} ergs cm^{-2} s^{-1} sr^{-1}. Therefore, the expected [O I] intensity is a few times 10^{-5} to 10^{-6} ergs cm^{-2} s^{-1} sr^{-1}. If diffuse [O I] emission associated with the diffuse [C II] emission is detected and is stronger than 10^{-5} ergs cm^{-2} s^{-1} sr^{-1}, the origin of the [C II] and [O I] line emissions can be attributed to the diffuse photodissociation regions.

The FILM is designed to survey the Galactic plane with higher sensitivity and to provide an accurate intensity maps of the [C II] and the [O I] line. We, therefore, expect that the FILM will reveal the origin of the diffuse [C II] emission.

2.2. *Physical Condition of Cirrus Clouds*

The *IRAS* discovered many infrared cirrus clouds at high Galactic latitudes (Low et al. 1984). The temperature and the optical depth of the dust in the cirrus clouds were derived from their far-infrared continuum spectra. However, since the cirrus clouds are thought to be far from a thermal equilibrium state between the gas and the dust, it is difficult to deduce the physical condition of the gas from that of the dust. Far-infrared atomic lines, such as [C II] 158 μm and [O I] 63 μm, can be good diagnostic tools to investigate the physics of the gas in the cirrus clouds.

Pottasch et al. (1979) derived, from the UV absorption line measurements, the result that the cooling rate by the [C II] line emission is 10^{-25} ergs s^{-1} per H atom. Gry, Lequeux, & Boulanger (1992) have reported a smaller but more scattered value for the [C II] cooling rate from a compilation of the UV measurements. Recently, the [C II] line emission from high-latitude clouds has been measured by a rocket-borne cooled spectrophotometer system (Bock et al. 1993). From the correlation with the H I column density, a [C II] gas cooling rate of $2.3(\pm 0.3) \times 10^{-26}$ ergs s^{-1} per H atom was derived. Using the above cooling rates, we estimate the [C II] line intensity of $(2–0.4) \times 10^{-6}$ ergs cm^{-2} s^{-1} sr^{-1} for a typical cirrus cloud with an H I column density of 2×10^{20} cm^{-2} corresponding to $A_v = 0.1$ mag.

According to Stark (1990), the expected [O I] intensity of the typical cirrus cloud is a few times 10^{-6} ergs cm^{-2} s^{-1} sr^{-1}, which is less than the detection limit of the FILM (see § 4.6).

The FILM has a high sensitivity so that the [C II] line emission from the cirrus clouds can be detected and could provide a clue to understand the excitation mechanism and the physical condition in the cirrus clouds.

2.3. *Search for Interstellar Shocks*

The [O I] 63 μm emission is theoretically expected to be strong in interstellar shocked gas (Draine, Roberge, & Dalgarno 1983; Hollenbach & McKee 1989). Interstellar shock waves are driven by various phenomena including stellar winds, cloud-cloud collisions, supernova explosions, and Galactic density waves. The [O I] emissions from such shocks have been detected (Cohen et al. 1988; Burton et al. 1990). According to the observational result on IC 443, a supernova remnant, by Burton et al., the [O I] 63 μm line intensity is expected to be $(8.0 - 0.7) \times 10^{-5}$ ergs cm^{-2} s^{-1} sr^{-1} for a FILM beam.

Draine et al. (1983) calculated the [O I] line intensity of 1×10^{-4} ergs cm^{-2} s^{-1} sr^{-1} from a C-shock wave with shock speed of 10 km s^{-1} into molecular gas with a density of 10^{2-4} cm^{-3}, a fractional ionization of 10^{-7}, and a magnetic field of 50 μG. This shock velocity is comparable with the velocity dispersion of the proper motion of the molecular clouds, and it can be expected, therefore, that such kinds of shocks generally occur in the Galactic plane. Therefore the FILM can detect the [O I] 63 μm emission from weak and diffuse shock waves, if a shocked area extends over a few arcminutes.

3. DESIGN OF THE FILM HARDWARE

3.1. *Optical System*

The FILM has a noble design in its optical system. It uses a "varied line-space cylindrically concave grating" which has been developed for the first time for the FILM. This grating allows us to achieve high throughput, reliability, moderately high resolution in the strict limits of small volume and light weight. All optical components as well as the grating itself are made of aluminum alloy by machining and are evaporated with gold.

Figure 1 shows the optical system of the FILM. At the focal plane of the IRTS, a small diagonal mirror is mounted for the FILM. The incident light from the telescope is reflected by 90 degrees and makes a focus on the input slit of the FILM. The slit is a rectangle of 1.4×3.5 mm whose elongated direction is perpendicular to the scanning direction of the IRTS. The light passes through the input slit with a F/4 divergence, is reflected by a plane mirror again, and is collimated by a cylindrical mirror in the Z-axis. The light diverging in the other direction reaches the cylindrically concave grating which has a ruling along the Z-axis.

After reflection and dispersion by the grating, the light goes back nearly along the path of the incident light and makes a focus at the front of the detector aperture. The location of the focus is shifted by 20 mm above that of the input slit in the Z-axis. The direction of the spectral dispersion at the focus is

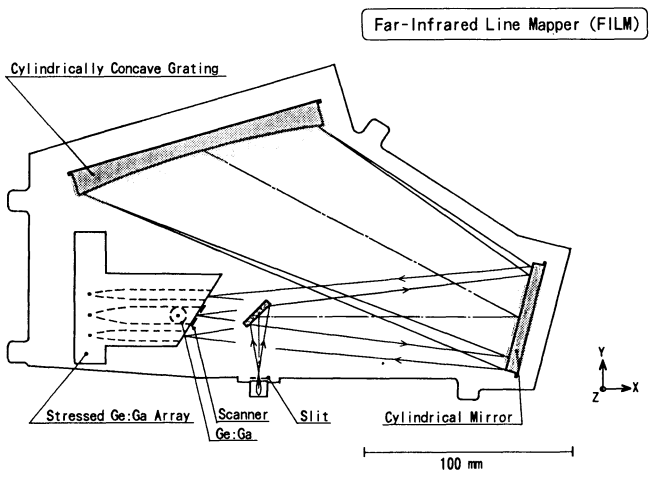

FIG. 1.—Schematic diagram of the FILM, viewed from behind the focal plane at the optical axis of the IRTS telescope. The converging beam to the detector mount is shifted from the diverging by 20 mm in the direction perpendicular to the sheet.

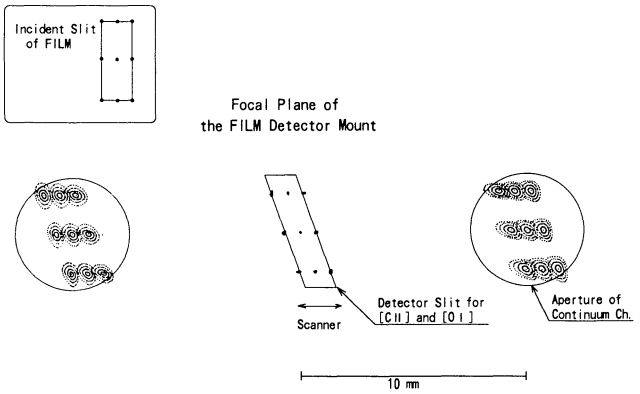

FIG. 2.—Ray trace of the FILM optical system. The shape of the incident rectangular slit is projected as a rhomboid at the focus in front of the detector mount. The residual aberration of the [C II] channel is very small as shown in the figure. The aberration of the continuum channels on both sides is larger but small enough compared to the FILM slit size and the diffraction limited image size.

along the Y-axis. The slit width of the detector aperture is the same as that of the input slit.

Conventional concave gratings which have envelopes of a part of a sphere do not need any collimator optics. However, in order to minimize the size in the perpendicular direction of the paper, we adopted a unique idea which uses a cylindrical mirror and a cylindrically concave grating. A result of a geometrical ray trace is shown in Figure 2. The aberration for the [C II] and the [O I] channels is much smaller than the slit size, which is nearly equal to the diffraction-limited image size for 158 μm. It is noted that the image of the rectangular shape of the input slit is deformed into a rhomboid.

The pitch of the grating was controlled so that the [C II] 157.7408 μm line is exactly equal to the second order light of the spectrometer. Then the [O I] 63.1837 μm line is almost the fifth-order light. The separation of the two lines at the focus is only 0.7 mm. The pitch surface of the grating is exactly a part of the cylinder but the ruling pitch is varied within $\pm 0.9\%$ in order to decrease the aberration. This grating has been made by Nikon for the FILM.

Figure 3 shows a schematic diagram of the filtering system of the FILM. A SrF_2 filter coated with diamond powder is used to block radiation at wavelength shorter than 50 μm. After the dispersion by the grating, lights of all orders near the blaze wavelengths are selected for the two line channels. Then, a KCl beam splitter reflects only fourth to six-order light to the [O I] channel, and an interference filter passes only fifth-order light. On the other hand, the light passing through the KCl beam splitter contains first to fourth and sixth orders of the light reflected by the grating. A Yoshinaga filter (Sakai, Nakagawa, & Yoshinaga 1968) passes only first and second orders and completely blocks higher order light. Because a stressed Ge:Ga detector cannot detect the first-order light (305 μm), only the second-order light (158 μm) is selected. The two continuum channels have a nearly identical filtering system with the [C II] channel except that they do not have a KCl beam splitter. Figure 4 shows the spectroscopic response for each channel and it can be seen that the blocking and order selections are complete.

3.2. *Detectors*

Detectors used in the FILM have been developed by a collaboration between ISAS and CRL (Hiromoto et al. 1992). A linear three element array of Ge:Ga photoconductor with a stress assembly is used for the [C II] 158 μm and the two continuum channels. On the other hand, a single element unstressed Ge:Ga photoconductor is used for the [O I] 63 μm channel. The two line channels have a common slit which is scanned in the direction of the spectral dispersion at 2 Hz by a spectral scanner. This mechanism allows us to extract the line intensity components from the total signals.

The light passing through the slit is divided into two spectral channels by a KCl beam splitter. Each beam is collected by a Winston cone collector into a detector cavity.

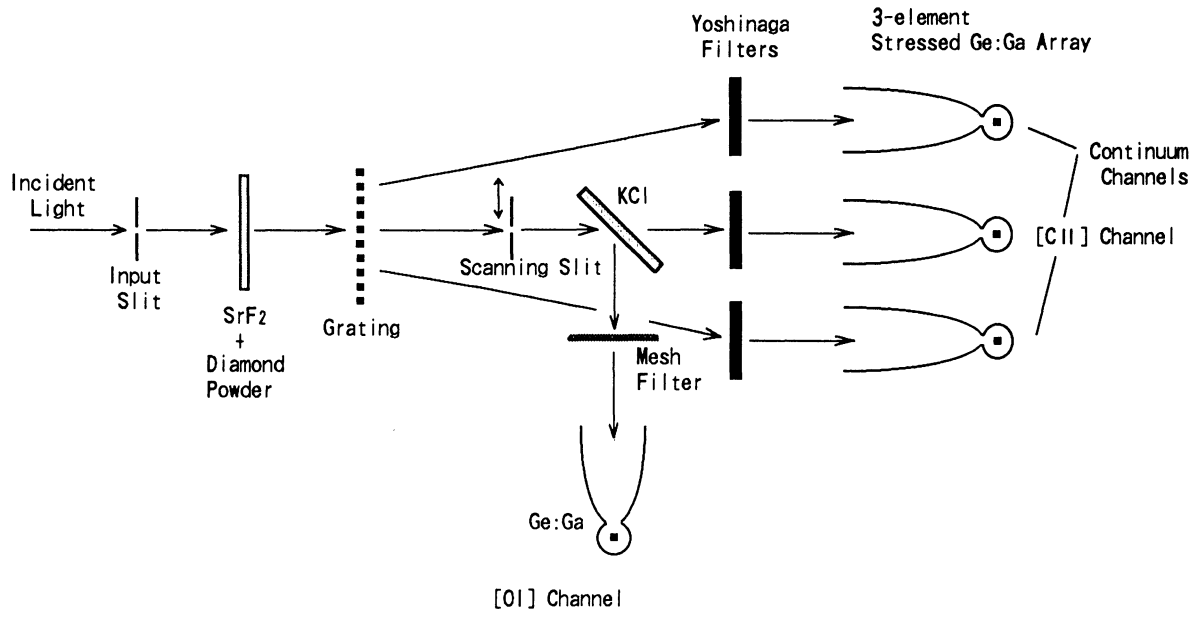

FIG. 3.—Schematic diagram of the filtering system

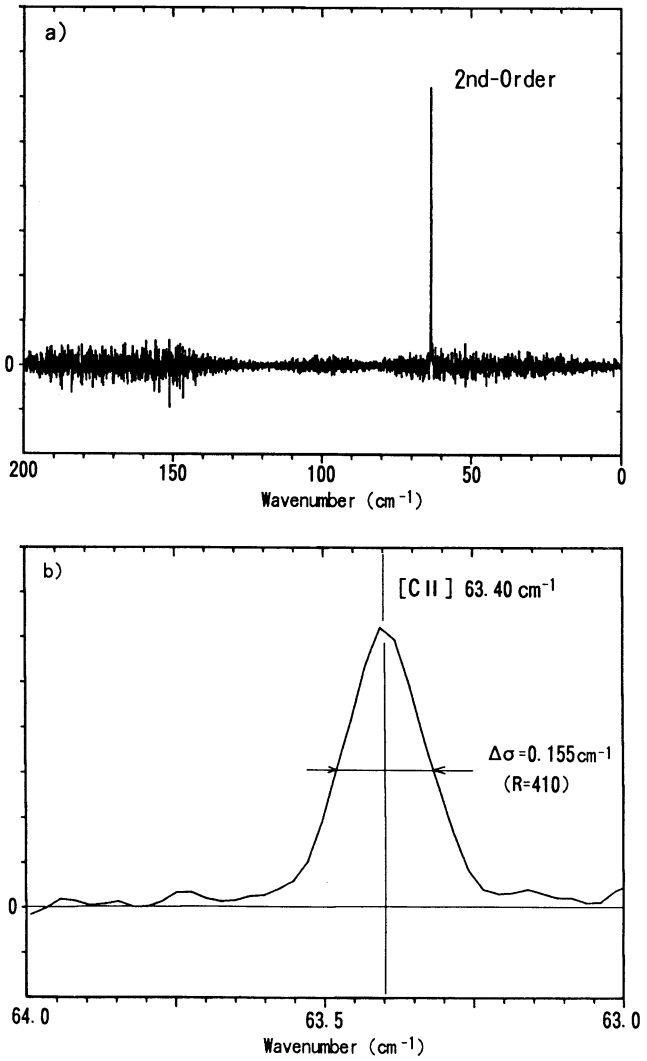

FIG. 4.—Results of the laboratory measurement of the spectral responses of the [C II] channel in a wide band (*a*) and in a narrow band near the [C II] line (*b*). The measurements were done by a Fourier transform spectrometer.

In order to stabilize the detector responsivities and suppress nonlinear responses, weak and constant light sources ("bias lights") are incorporated to the detector assembly. The lights are introduced from the sources through thin stainless steel pipes into the detector cavities. They can be continuously turned on during observations in order to reduce the dependence of the responsivity on the total incident flux. When this light is on, the responsivity change caused by the total flux change should decrease, but the photon noise would slightly increase under a lower total flux condition described below.

It has been pointed out that performance of detectors is also affected by cosmic high-energy particles (Oda, Lemke, & Wolf 1984). During the *IRAS* mission, cosmic rays hit on each detector at the rate of about one per 20 seconds (*IRAS* Explanatory Supplement 1985). Because the volume of the detector element (0.125 mm^3) is less than one-tenth of that of the *IRAS* (2 mm^3) and because the orbital altitude is 482 km while the *IRAS* is into 900 km, the rate of cosmic rays' hits will be much smaller than that of the *IRAS*. Except for passage through the South Atlantic Anomaly (SAA), the hit rate is estimated to be about one event in 10 minutes. For annealing the radiation effect after passing through the SAA, the detector bias voltage can be increased above the breakdown voltage ("bias boosting").

3.3. *On-Board Electronics*

The first stage of each sensor channel is a conventional transimpedance amplifier (TIA). Four JFETs (Infrared Laboratories, Inc.) are mounted near the detectors. The TIA method has an advantage of a wide dynamic range, which covers both the bright Galactic plane and faint cirrus clouds.

After passing a low-pass-filter, the signal voltage is converted by a square-root amplifier, by which the dynamic range can be increased significantly in the photon noise limited condition without any degradation of the signal to noise ratio. The resultant dynamic range can be about 10^8 with a 16 bit A/D converter without any electronics for changing gains.

The detector bias voltages are changeable in order to optimize operating conditions of the detectors and apply high voltages to them for quick recovery after the passage of cosmic particles through the detector.

4. LABORATORY TESTS

We have measured the performance of the FILM, and have confirmed that it has excellent performance as designed. For almost all the tests, the FILM was mounted on the focal plane of the IRTS flight telescope. Part of the spectroscopic performance of the FILM was measured before being mounted on the telescope. The results of these measurements are summarized in Table 1.

4.1. *Responsivity*

For a DC responsivity measurement of the FILM detector, we used a neutrally attenuated blackbody source attached in front of the telescope aperture. It is a copper disk coated with a special black paint (Bock & Lange 1993) and has a thermometer, a heater for temperature control, and a mask with grid-patterned holes for suitable attenuation.

In the source temperature range between 20 and 70 K, the measured responsivities of the FILM detectors were constant within 10%. The results are shown in Table 1. The values of the responsivity listed in the table include all unknown losses; known losses are included in the optical throughput. Comparing this responsivity with those measured prior to the installation on the telescope, there remain discrepancies of a factor of 2 at most. These discrepancies have not been resolved. As for the absolute responsivity, observations of astronomical objects whose fluxes have been measured previously will provide a good calibration.

Since the detectors of the FILM are photoconductors, there may be responsivity changes due to changes of the total incident flux and the temperature, and a transient response caused by a stepwise change of the incident flux. First, the change of the responsivity due to the temperature change was less than 5% between 1.75 and 2.0 K; the expected detector temperature in orbit is 1.8–1.9 K. Second, measured DC responsivities were constant within 10% under the total incident flux less than 10^9 photons per second, which corresponds to the sky brightness of less than 100 GJy sr^{-1}. Third, as shown by Hiromoto et al. (1992), the AC responsivities of the detectors (Channels 1, 2, and 3) depend on the total incident flux. It was found that the change of signal voltage after the calibration lamps turn on depends on incident radiation flux. Figure 5 shows examples of

TABLE 1

FILM SUMMARY

A.

Parameter	Value
Size (mm)	250 × 150 × 130(H)
Weight (g)	1950
Grating	a varied line-space cylindrically concave grating
Beam size (FWHM)	8′ (dispersion direction) × 13′
Area to be observed	10%–20% of the sky

B.

	Channel			
Parameter	1	2	3	4
Band Center (cm^{-1})	64.4	63.4[a]	62.4	158.4[b]
Resolving Power	130	409	130	405
Detectors	(linear 3-el. stressed Ge:Ga array)			Ge:Ga
Optical through-put[c]	0.34	0.30	0.34	0.15
S(detector) (A/W)[d]	10.1	11.1	9.7	0.51
System NEP (10^{-16} W $Hz^{-1/2}$)	1.8	0.60	1.7	12

[a] Scanning range is 63.2–63.6 cm^{-1}.
[b] Scanning range is 157.9–158.9 cm^{-1}.
[c] Calculated efficiency of the FILM optics including filters.
[d] Including all unknown loss.

the slower and nonlinear responses for a signal change under various conditions of the total incident flux.

The FILM has two calibration lamps in order to correct any changes of the responsivities during the observation, including the effect caused by background radiation. The calibration light generates a rectangular pulse of 2 seconds every 64 seconds. Since the rectangular signal includes higher frequency components, the measured calibration signal is affected by the AC responsivity change due to the total flux change described above. However, it was found that, using laboratory measurements, this effect can be corrected with a residual error of 10%.

4.2. *Noise*

Measured noise voltages of all channels are nearly proportional to a square root of the detector current when the photon flux is high (1 GJy sr^{-1}), and otherwise are nearly constant. The continuum brightness of 1 GJy sr^{-1} corresponds to that of the bright ridge of the Galactic plane. In a dark condition, the measured noise is a few times larger than the expected thermal noise of the feedback resistor. This enhancement is caused by electrical interferences and by a photon noise of an unidentified light source in the FILM. The surface brightness at high Galactic latitudes is on the order of 10 MJy sr^{-1}. Therefore, the noise and the resultant system noise-equivalent-power (NEP), shown in Table 1, will be nearly constant except near the Galactic plane.

4.3. *Spectral Characteristics*

Spectral characteristics of the FILM have been measured using a Fourier transform spectrometer before the installation on the IRTS flight telescope. The spectra resolution and the central wavenumber of each detector channel are shown in

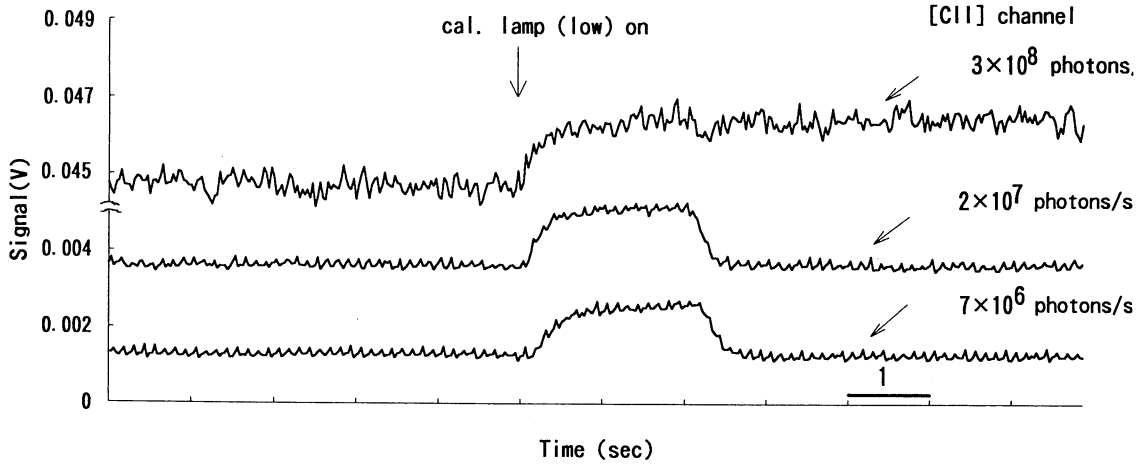

FIG. 5.—Signal output (the [C II] channel) of one of the calibration lamps under three different backgrounds. The lowest DC level was achieved by making the shutter closed, the middle and highest level by turning each of the bias lamps on. In case of the lowest and middle level, the calibration lamp was activated for 2 seconds. The spectral scanning was not active.

Table 1, which are just as designed. As shown in Figure 4, we can see no diffuse spectral component, which would be mainly caused by the stray light in the spectrometer system. The diffuse spectral component obtained is less than 10^{-3} of the second-order light, and therefore its effect should be quite small.

The performance of spectral scan of the [C II] channel (Channel 2) was measured. At the measurement, the FILM was mounted on the IRTS telescope, and a parallel beam from a spectral line source whose wavelength is equal to the [C II] line was introduced into the IRTS. The scan worked correctly as designed. As for the spectral scan of the [O I] channel (Channel 4), it is also expected to work properly, because the aperture slit is common for Channels 2 and 4.

4.4. *Instrumental Polarization*

Because the FILM is a grating spectrometer, a certain degree of instrumental polarization was expected. The instrumental polarization was measured for Channels 1 and 2 by using a polarized source. Both channels have instrumental polarization of 25% along the direction parallel to the ruling of the grating. However, because the [C II] 158 μm and the [O I] 63 μm lines are predominantly emitted by spontaneous transitions from collisionally excited states, it can be assumed that the line emissions have no polarization.

On the other hands, the continuum emission may have a small polarization, of the order of 1%. Therefore, the instrumental polarization will introduce an error of less 1% into the continuum channels.

4.5. *Beam Size*

The beam pattern of the FILM mounted on the IRTS was measured for Channels 1, 2, and 4. The beam pattern is nearly elliptical and the FWHM is 8 arcmin along the dispersion direction and 13 arcmin along the scanning direction. Observations of point-like sources in orbit will provide another accurate measurement of the beam pattern.

4.6. *Sensitivity and Comparison with Other Instruments*

On the basis of those measurements described above, we have calculated the detection limits for the two spectral lines under low background radiation. The results are shown in Figures 6 and 7. In these figures, the intensities from typical astronomical objects and the detection limits of other instruments are also shown.

The 3 σ detection limit of the [C II] channel is 1×10^{-6} ergs cm^{-2} s^{-1} sr^{-1}, which is one to two orders of magnitude better than those of the air-borne and balloon-borne telescopes. The diffuse [C II] emission from the Galactic plane, which is one of main observational targets, will be detected with a high signal-to-noise ratio ($\sim$100). Moreover, the FILM is expected to detect a weak [C II] emission from regions outside the Galactic plane.

The FIRAS on the *COBE* has measured the extended [C II] emission (Wright et al. 1991), but the beam size of 7° is too large to distinguish the individual Galactic components from the general Galactic plane component in the [C II] intensity map of the whole sky. By contrast, it is expected that the FILM can resolve those components with its smaller beam size of 8 × 13 arcminutes.

The FILM also has an advantage over the LWS on the ISO (ISO Scientific Capabilities of the ISO Payload 1991) in observing the [C II] emission from sources which extend over 10 arcminutes.

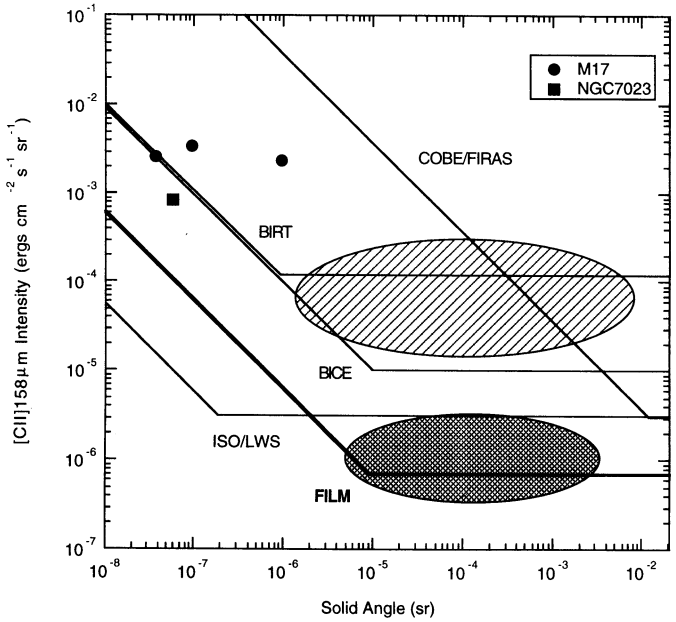

FIG. 6.—Sensitivity of the [C II] channel of the FILM (3 σ, 1 FOV), compared with those of BICE (3 σ, 1 FOV) (Nakagawa et al. 1993), BIRT (3 σ, 1 FOV) (Shibai et al. 1991), FIRAS on *COBE*, and LWS on ISO (3 σ, integration time is 1 s) (Scientific Capabilities of the ISO Payload 1991). The detection limit of the FIRAS is an approximate estimate using the all-sky [C II] 158 μm map of Wright et al. (1991). The limit of the ISO/LWS is inversely proportional to the square root of the integration time. The observed or estimated intensities of some astronomical sources are also shown. *Hatched region:* diffuse [C II] emission from the Galactic plane (see § 2.1). *Shaded region:* cirrus clouds (see § 2.2).

However, as for the detection limit of the [O I] channel, it is 3 times worse than that of the ISO-LWS. The FILM will survey about 10% of the entire sky with these detection limits, where the ISO-LWS is expected to concentrate mainly on mapping and resolving of small-scale structures. Therefore, the FILM and ISO-LWS can be a complementary pair of far-

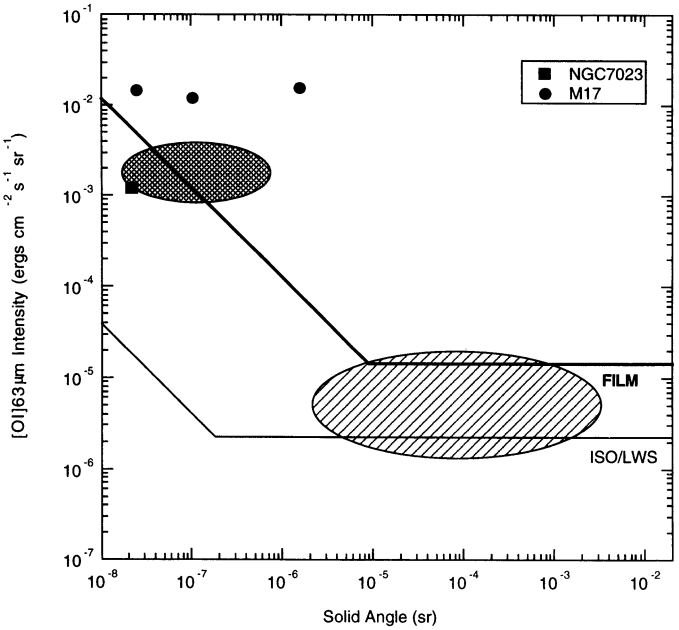

FIG. 7.—Same as Fig. 6, except for the [O I] channel. *Hatched region:* expected diffuse [O I] emission from the Galactic plane (see § 2.1). *Shaded regions:* shocked gas (see § 2.3).

infrared spectroscopic instruments, not only for the [O I] line but also for the [C II] line.

5. SUMMARY

The Far-Infrared Line Mapper (FILM) on the Infrared Telescope in Space (IRTS) has been developed and tested in the laboratory. The FILM will simultaneously measure the [C II] 158 μm and [O I] 63 μm line intensities with high sensitivity for extended sources and spatial resolution of 8 arcmin × 13 arcmin, and provide intensity maps over 10% of the sky. Investigations of diffuse [C II] emission from the Galaxy, infrared cirrus clouds, and the cooling process of interstellar clouds will be significantly advanced by the FILM.

Many people at ISAS have contributed to the development of the FILM, including M. Narita and other members of IR group at ISAS. Among them, Mrs. Y. Yamashita Yui fabricated an excellent low-pass filter for the FILM. K. Okumura and H. Yano assisted us at the laboratory calibration of the FILM. We have been supported technically by Professor H. Ishimoto at University of Tokyo for making a high thermal conductive copper, by S. M. Smith at NASA/ARC for providing a black coating, by Mitaka Kohki for machining the complex FILM structure, and by Nikon for developing a unique grating. We specially thank T. Matsumoto, H. Murakami, T. Onaka, and other members of IRTS project.

REFERENCES

Bock, J., et al. 1993, in AIP Conf. Proc. No. 278, Back to the Galaxy, ed. S. S. Holt & F. Verter (New York: AIP), 299
Bock, J., & Lange, A. E. 1993, preprint
Burton, M. G., Hollenbach, D. J., Haas, M. R., & Erickson, E. F. 1990, ApJ, 355, 197
Cohen, M., Hollenbach, D. J., Haas, M. R., & Erickson, E. F. 1988, ApJ, 329, 863
Cooksy, A. L., Blake, G. A., & Saykally, R. J. 1986, ApJ, 305, L89
Doi, Y., Nakagawa, T., Yui, Y. Y., Okuda, H., Shibai, H., Nishimura, T., & Low, F. J. 1993, in AIP Conf. Proc. 278, Back to the Galaxy, ed. S. S. Holt & F. Verter (New York: AIP), 307
Draine, B. T., Roberge, W. G., & Dalgarno, A. 1983, ApJ, 264, 485
Gry, C., Lequeux, J., & Boulanger, F. 1992, A&A, 266, 457
Hiromoto, N., Itabe, T., Shibai, H., Matsuhara, H., Nakagawa, T., & Okuda, H. 1992, Appl. Optics, 31, No. 4, 460
Hollenbach, D., & McKee, C. 1989, ApJ, 342, 306
Hollenbach, D. J., Takahashi, T., & Tielens, A. G. G. M. 1991, ApJ, 377, 192
IRAS Catalogs and Atlases: Explanatory Supplement. 1988, ed. C. A. Beichman, G. Neugebauer, H. J. Habing, P. E. Clegg, & T. J. Chester (Washington, DC: GPO)
ISO Scientific Capabilities of the ISO Payload. 1991, ISO-SSD-8805, Issue 1.0, ESA
Lange, A. E., Freund, M. M., Sato, S., Hirao, H., Matsumoto, T., & Watabe, T. 1994, ApJ, 428, 384
Low, F. J., et al. 1984, ApJ, 278, L19
Matsuhara, H., et al. 1992, in Chemistry and Spectroscopy of Interstellar Molecules, ed. D. K. Bohme, E. Herbst, N. Kaifu, & S. Saito (Tokyo: Univ. Tokyo Press), 277
Murakami, H., et al. 1994, ApJ, 428, 354
Nakagawa, T., et al. 1993, in AIP Conf. Proc. 278, Back to the Galaxy, ed. S. S. Holt & F. Verter (New York: AIP), 303
Noda, M., Matsumoto, T., Matsuura, S., Noguchi, K., Tanaka, M., Lim, M. A., & Murakami, H. 1994, ApJ, 428, 363
Oda, N., Lemke, D., & Wolf, J. 1984, Int. J. Infrared Millimeter Waves, 5, No. 11, 1499
Okuda, H., et al. 1989, in IAU Symp. 136, The Center of the Galaxy, ed. M. Morris (Dordrecht: Reidel), 145
Pottasch, S. R., Wesselius, P. R., & van Duinen, R. J. 1979, A&A, 74, L15
Roellig, T., Onaka, T., McMahon, T., & Tanabé, T. 1994, ApJ, 428, 370
Sakai, K., Nakagawa, Y., & Yoshinaga, H. 1968, Jpn. J. Appl. Phys., 7, 792
Shibai, H., et al. 1991, ApJ, 374, 522
Stacey, G. J., Visuso, P. J., Fuller, C. E., & Kurtz, N. T. 1985, ApJ, 289, 803
Stark, R. 1990, A&A, 230, L25
Tielens, A. G. G. M., & Hollenbach, D. 1985, ApJ, 291, 722
van Dishoeck, E. F., & Black, J. H. 1988, ApJ, 334, 771
Wright, E. L., et al. 1991, ApJ, 381, 200
Zink, L. R., Evenson, K. M., Matsuhima, F., Nelis, T., & Robinson, R. 1991, ApJ, 371, L85